

RESEARCH ARTICLE

Spectrally and angle-resolved emission of thin film fluorescence collectors

Hendrik Sträter^{1*}, Sebastian Knabe¹, Thomas J.J. Meyer² and Gottfried H. Bauer¹¹ Institute of Physics, Carl von Ossietzky University Oldenburg, D-26111 Oldenburg, Germany² Teknova, Gimlemoen 19, 4630 Kristiansand, Norway

ABSTRACT

Fluorescence collectors (FSCs) offer the possibility to collect and concentrate direct and ambient light and are, thereby, an option to decrease the cost of high-efficiency solar modules. So far, scattering, absorption and reabsorption of the incoming and fluorescence light cannot be discriminated completely in experiments. Thus, the contribution to the discrepancy of experimentally achieved efficiencies from the theoretical one has not been identified. To understand the propagation of the fluorescence light by illumination at a certain distance from the edge of the FSC, we have developed a two-dimensional analytical model based on geometrical optics that reproduces the experimental results. Under certain conditions for each distance from the edge regimes of detection angles exist for which no fluorescence light of the edge occurs. Copyright © 2011 John Wiley & Sons, Ltd.

KEYWORDS

solar concentrator; fluorescence concentrator; fluorescence collector; scattering

*Correspondence

Hendrik Sträter, Institute of Physics, Carl von Ossietzky University Oldenburg, D-26111 Oldenburg, Germany.

E-mail: hendrik.straeter@uni-oldenburg.de

Received 11 April 2011; Revised 3 August 2011; Accepted 16 September 2011

1. INTRODUCTION

Solar fluorescence collectors (FSCs) convert solar photons of a particular energy range of direct or indirect incident light into photons with lower energies [1,2]. This is performed by absorption of the light by a dye in a dielectric matrix and Stokes-shifted fluorescence emission. In theory, the main part of the emitted fluorescence photons is conducted to the edges of the FSC by total internal reflection due to the contrast in refractive indices of the FSC and its environment. Across the comparably small area of the edge, fluorescence photons, which have been generated by solar photons entering through a conveniently large FSC light entrance area, are coupled to appropriate band gap solar cells. The gain factor of an FSC is given by the ratio of the front surface to the edge surface and the number of assembled solar cells at the edges. The losses of fluorescence photons led to the solar cell resulting from incomplete conversion of solar light into fluorescence, leak of fluorescence photons through the escape cone, reabsorption of fluorescence photons due to spectral overlap of absorption and emission of the dye and subsequent incomplete photon recycling and repeated

emission through the escape cone. In addition, photons leave the FSC because of inelastic and elastic scattering at non-ideal flat surfaces and in the bulk. For the identification of losses and for characterization of the performance of two different designs of FSCs, we have measured the fluorescence light at the edges and at the rear surface with different types of illumination, such as lateral homogeneous excitation, or local selective illumination as a function of distance from the edge.

2. EXPERIMENTS

We have studied the light emission of two FSC designs: an FSC [2] consisting of a 1-mm-thick poly(methyl methacrylate) (PMMA) substrate with homogeneous depth-dependent Lumogen F Rot 305 dye concentration (BASF AG Veredlungchemikalien für Lacke, Kunststoff und Spezialitäten 67056 Ludwigshafen, Deutschland) and an FSC consisting of a glass substrate with a thin film of Rhodamine 6G (Rh6G) dye embedded in a PMMA matrix at the top surface of a 1-mm-thick glass substrate, as investigated in [3,4]. We used two FSC samples with dye concentrations 0.3

and 0.8 g/L denoted by “FROT1” and “FROT2”, respectively. The exact dye concentration of the Rh6G sample (denoted by “Rh6G”) is not known. Because we do not compare the overall efficiency of both FSC designs, the difference in dye concentration as well as the fact that we use two different fluorescence dyes can be neglected.

The experimental setup is outlined in Figure 1. The excitation has been performed by an Ar⁺ laser (488 nm), which is focused by a cylindrical lens and a slit aperture onto the front surface of the FSC via a mirror on a translation stage to provide for the excitation at different and adjustable distance from the FSC’s edges. For homogeneous illumination to be provided, the slit aperture is replaced by a diffuser plate. The photons emitted from the FSC for the rear surface as well as for the edge are collected in a rotatable collimator that feeds the photons through a glass fiber to a liquid nitrogen-cooled optical multichannel analyzer (InGaAs-OMA) for wavelength resolution. To obtain the so-called “first generation fluorescence”, the fluorescence with minimal reabsorption, we collected the fluorescence at the rear surface through an aperture in the substrate holder. Because of the design of the substrate holder, we are limited to detection angles of $0^\circ \leq \beta \leq 70^\circ$. The collimator is carefully focused on the center of the edge of the FSC providing for a resolution of the collimator of $\beta \approx 1^\circ$.

3. EXPERIMENTAL RESULTS

Figure 2(a–d) shows the measured photon fluxes through the Rh6G FSC’s edge as a function of detection angle β and wavelength λ for illumination at several distances from the edge $d = 1.0, 3.5, 9.8$ and 19.9 mm. For each of the values d , angles $\beta(d)$ for which no light is detected, are observed resulting in a fringe-like pattern. With increasing angle β and thus with increasing light path of the photons

within the FSC, the intensity decreases obviously because of absorption according to Lambert–Beer’s law, incomplete photon recycling and also due to scattering.

The fringe-like pattern vanishes under homogeneous illumination as shown in Figure 3(a). The fluorescence increases with increasing detection angle to a maximum at $\beta \approx 18^\circ$ and decreases with further ascending detection angle. For small angles, almost no fluorescence can be detected. The normalized fluorescence spectra for detection angles $\beta = 7^\circ$ and 60° are shown in Figure 3(b). A small shift to lower photon energies can be recognized. In Figure 3(c), the “first generation” spectrum is compared with the fluorescence spectra measured at the FSC’s edge for different detection angles β and under homogeneous illumination. With increasing detection angle β , the photon flux at the edge slightly decreases, whereas the loss of fluorescence photons, especially in the low energy regime, is tremendous compared with the “first generation” fluorescence. Figure 3(d) shows the spectra for different points of illumination and detection angle $\beta = 45^\circ$. It can be seen that the spectra are red shifted with increasing distance to the edge and decrease because of reabsorption and scattering. Nevertheless, the red shift due to the change of detection angle is negligible compared with the red shift caused by the variation of parameter d , which designates the distance from the edge.

Both FROT samples show a slightly different behavior. Because the fluorescence dye is homogeneously distributed within the FSC, one would expect that under all angles fluorescence light can be detected. In Figure 4, the measured fluorescence at the edge as a function of detection angle β under illumination at $d = 14$ mm is shown. For both samples, a modulation of the edge fluorescence is observed, with the modulation being larger for the sample FROT2 with higher dye concentration compared with the sample FROT1. This effect can be understood by a shift of the absorption profile

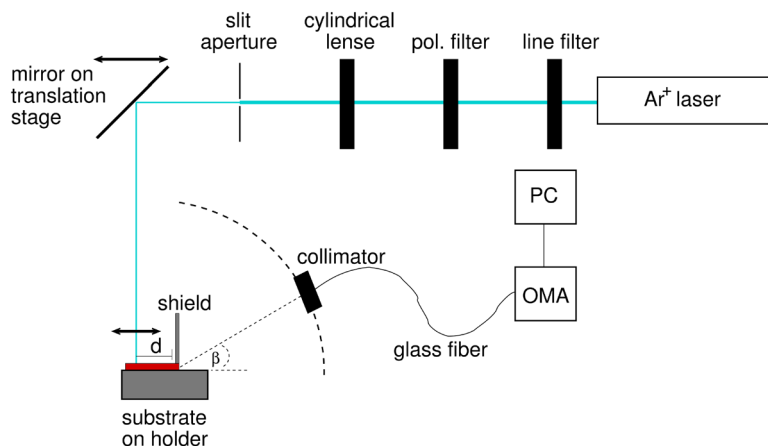


Figure 1. Experimental setup for the detection of fluorescence light coming out of the edge as a function of detection angle and wavelength. A slit illumination is used to ensure a constant photon flux along the fluorescence collector. The distance to the edge is adjusted by a mirror on a translation stage.

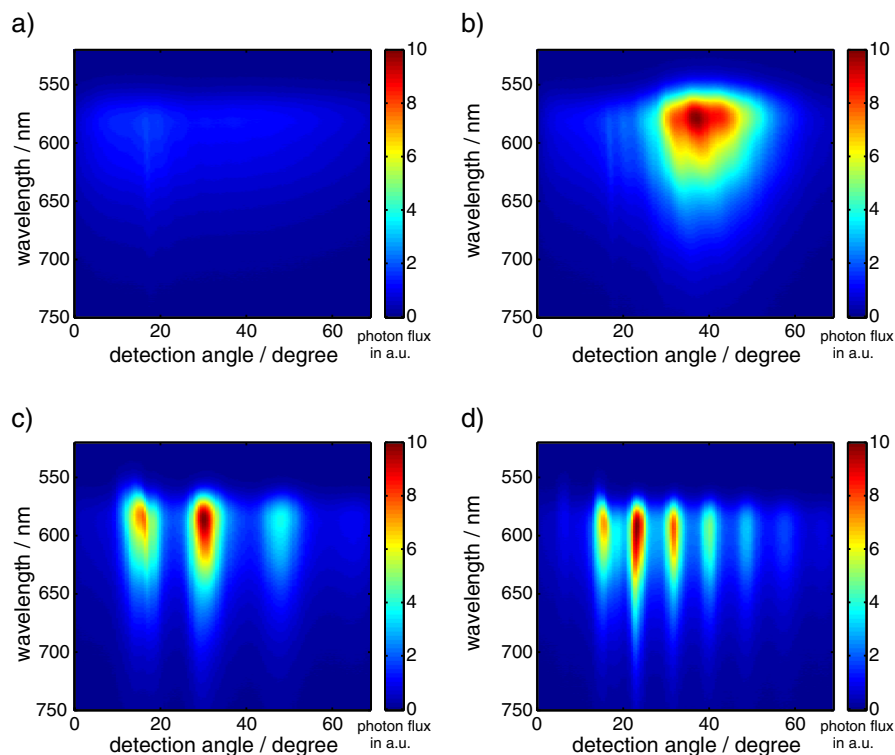


Figure 2. Photon fluxes from the edge of a Rh6G fluorescence collector as a function of detection angle β and wavelength λ for different distances d . For illumination near the edge, almost no fluorescence can be detected. With increasing distance, a fringe pattern occurs, with increasing number of fringes and decreasing width of each fringe. Because the light path becomes longer with the detection angles, less fluorescence can be detected for higher detection angles.

of the incoming light, which is believed to be similar to the emission profile of the luminescence toward the front side. A reduction of the extension of emitting volume, for example, to a thin layer close to the top of the FSC leads to a stronger selection of angles, under which the fluorescence light escapes through the edge. For very high dye concentrations, most of the fluorescence is emitted in the first layers of the FSC, and the FROT2 sample behaves qualitatively, similar to the Rh6G sample.

Similar observations have been presented and discussed in [5] for fluorescence collectors with homogeneously embedded dye. Because the sample in [4] is illuminated homogeneously, the presented angle-selecting behavior holds only for very small angles as shown in Figure 3(a).

For determination of the effect of scattering at non-perfect surfaces and dye molecules within the PMMA matrix and the PMMA matrix itself, respectively, the normalized fluorescence for a wavelength with large Stokes shift is shown in Figure 5 for both sample designs. Because of the large Stokes shift, we assume no reabsorption of fluorescence. With increasing d and β , the fluorescence at the edge decreases for all samples. Nevertheless, the relative loss of photons in the Rh6G sample is larger than in both FROT samples, which more or less show the same behavior. Because we can assume that the quality

of the surfaces of the FROT samples is the same, the higher loss of photons with increasing detection angle or distance to the edge is due to scattering at the surface of the Rh6G sample.

4. NUMERICAL REPRODUCTION OF LIGHT PROPAGATION IN AN FSC

We consider a rectangular glass substrate ($25 \times 25 \times 1$ mm) overcoated with a thin film of dye embedded in a polymer matrix. The refractive indices of the matrix and the substrate are almost equal, and therefore both denoted by n_{FSC} , whereas the refractive index of the ambient air is $n_0 < n_{\text{FSC}}$.

The substrate is illuminated monochromatically at a spot with width $s < d$ (d is the distance from the edge). Because the orientation of elongated dye molecules is assumed to be distributed randomly, the fluorescence light is emitted isotropically into the solid angle 4π . The emitted fluorescence light travels to the surface both at the top and at the bottom of the FSC, where it obeys Fresnel's law and Snellius' law for reflection and transmission. In our approach, we neglect the influence

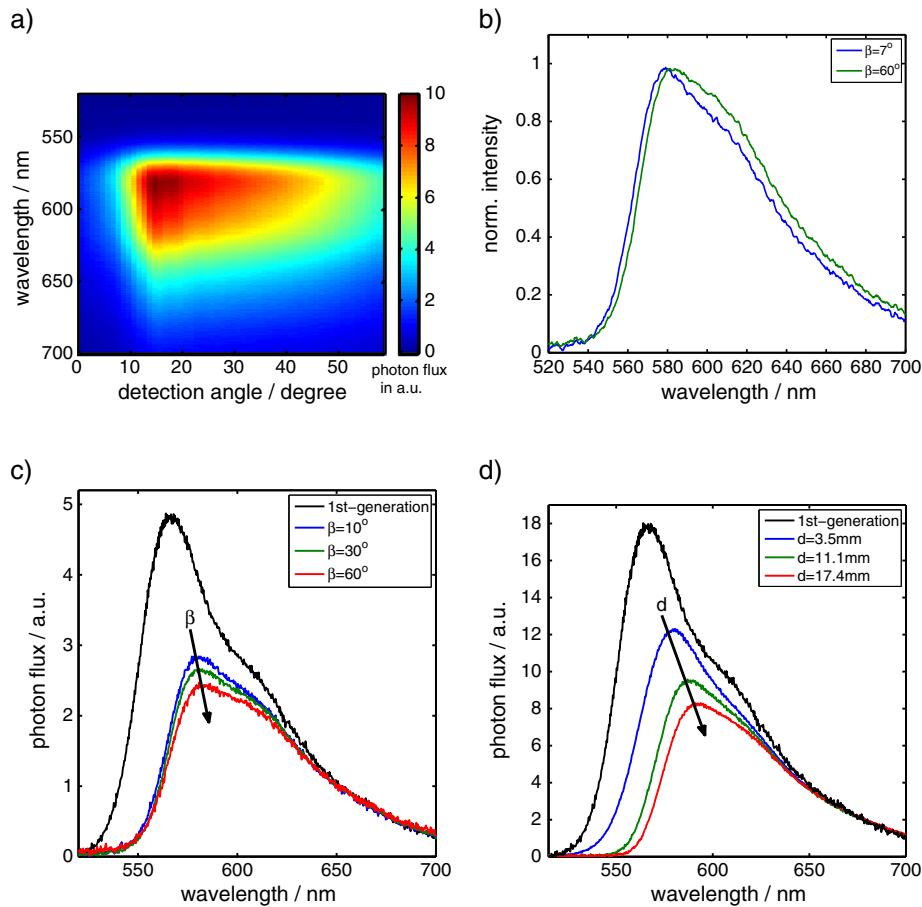


Figure 3. (a) Photon flux from the edge of the Rh6G sample as a function of detection angle β and wavelength λ for homogeneous illumination. (b) Normalized photon flux from the edge of the Rh6G sample for detection angles $\beta = 7^\circ$ and 60° . (c) Photon flux of the edge fluorescence for various detection angles β under homogeneous illumination compared with the first generation fluorescence. (d) Photon flux as a function of illumination point at $\beta = 45^\circ$.

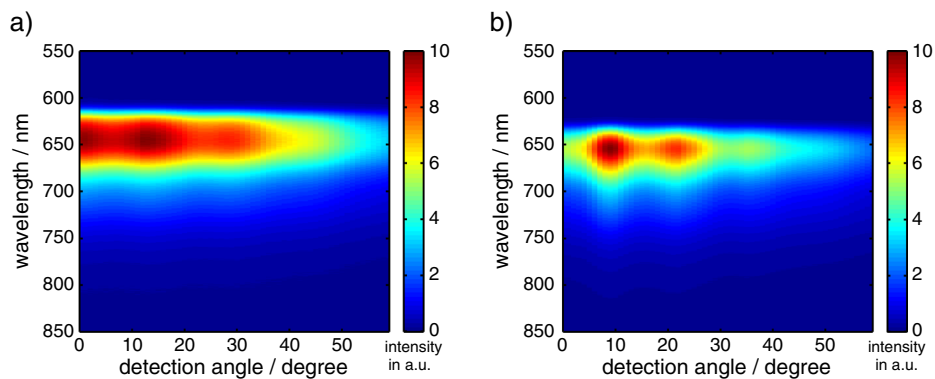


Figure 4. Photon fluxes from the edge of fluorescence collector samples (a) FROT1 and (b) FROT2 as a function of detection angle β under point-wise illumination with distance to the edge $d = 14$ mm.

of Fresnel's law. In this case, the light is refracted under the detection angle

$$\beta = \arcsin\left(\frac{n_{\text{FSC}}}{n_0} \sin\theta\right) \quad (1)$$

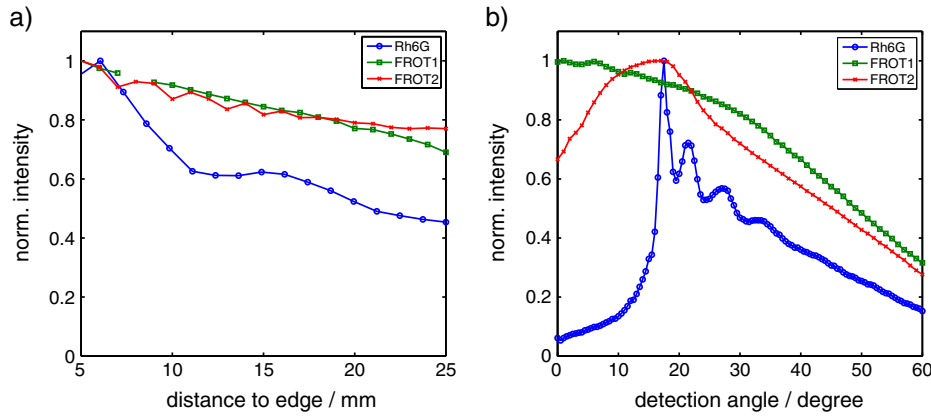


Figure 5. (a) Normalized fluorescence from the edge accumulated over all detection angles ($0 \leq \beta \leq 60^\circ$) as a function of distance of illumination d . (b) Normalized fluorescence accumulated over all distances ($0 < d \leq 25$ mm) as a function of detection angle β .

with θ the angle under which the light is emitted into the glass substrate. Keep in mind that the emission angle θ is defined to the normal of the edge for simplification.

Although for $\theta > \theta_{c,t} = \arccos(n_0/n_{\text{FSC}})$, the emitted light leaves the FSC through the front surface, for $\theta_{c,e} < \theta < \theta_{c,t} = \arcsin(n_0/n_{\text{FSC}})$, the light undergoes total internal reflection at the edge of the FSC and is guided back into the FSC. Only for $\theta < \theta_{c,e}$ the light can leave the FSC at the edge.

The totally reflected light leaves the FSC through the edge either from the bottom side (index b) or from the top side (index t) of the edge. All other possible paths lie within these limiting cases and are not included in the calculation. This situation is sketched in Figure 6.

For a given position d of illumination, the emission angles under which light can be detected are

$$\theta_b = \arctan\left(\frac{h(2m+1)}{d}\right) \quad (2)$$

and

$$\theta_t = \arctan\left(\frac{2h(m+1)}{d}\right) \quad (3)$$

with h the height of the FSC and $m = -m_{\text{max}}-1, \dots, m_{\text{max}}$ a parameter connected to the order of total internal reflections in the FSC. Negative orders m corresponded

to negative detection angles. Obviously for this model, a change of the dye from the top to the bottom of the FSC is equivalent with the exchange of θ_t and θ_b . The maximum order of total reflections m_{max} is given by the critical angle $\theta_{c,e}$:

$$m_{\text{max}} = \left\lfloor \frac{d \tan \theta_{c,e} - h}{2h} \right\rfloor \quad (4)$$

Because of the limited co-domain of the arctan, for any given position d of illumination there exist detection angles β , which are not accessible algebraically. For these angles, no light can be detected. In Figure 7, the gray regions represent the regions of detection angles β corresponding to Equation (1) for a 1-mm-thin substrate as a function of the distance of illumination.

Because of the very thin layer of fluorescence dye, the direct emission of the layer toward the collimator can be neglected. Therefore, we can define a minimum detection angle for homogeneous illumination given by

$$\beta_{\text{min}} = \arcsin\left(\frac{n_{\text{FSC}}}{n_0} \frac{h}{l}\right) \quad (5)$$

with l the total length of the FSC, as well as a minimum distance for spatially selected illumination given by

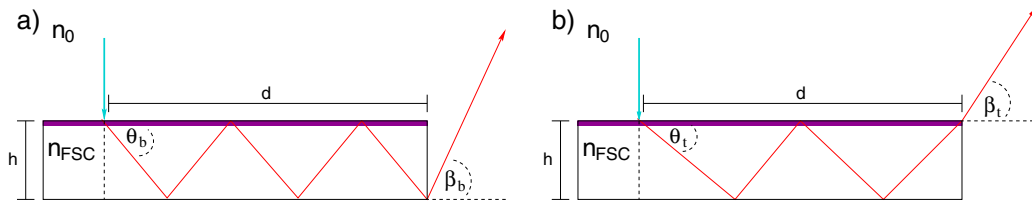


Figure 6. Light propagation within a fluorescence collector (FSC) by total internal reflection and refraction at the edge. The illumination is performed point-wise and perpendicular to the surface at a certain distance d from the edge. For simplicity, we are only interested in the fluorescence light that leaves the FSC (a) through the bottom of the edge or (b) through the top of the edge.

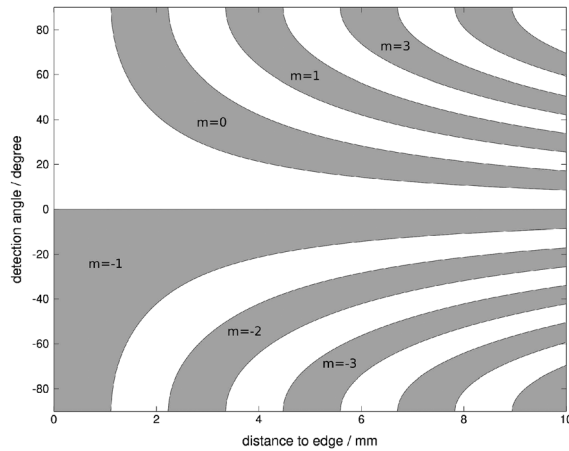


Figure 7. Angles β (gray area) for which light is detected as a function of the distance of illumination d . The patterns for orders m do not overlap. The emission angles into the upper and lower halves are complementary to each other.

$$d_{\min} = \frac{h}{\tan \theta_{c,e}} \quad (6)$$

under which light can be detected. The existence of a minimum detection angle can be verified because the fluorescence for low angles as shown in Figure 3(a) is negligible.

Figure 8 shows the fluorescence at the edge for a constant wavelength as a function of detection angle β and distance to the edge d for a thin film FSC. The black lines indicate the regimes given by Equations (2) and (3).

We assume that the emitted fluorescence photon flux decreases because of elastic scattering at non-perfect surfaces as well as because of elastic scattering at dye molecules within the PMMA matrix. From the experimentally determined fluorescence at different illumination positions d and detection angles β , it is possible to separate surface scattering from bulk scattering. For simplification we define a variable

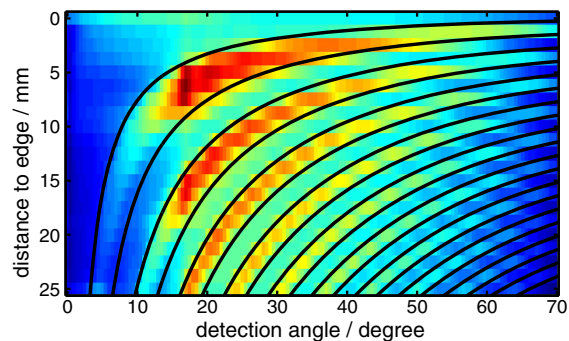


Figure 8. Fluorescence at the edge of the thin film fluorescence collector for a constant wavelength as a function of detection angle β and illumination point d . The black lines separate the areas where light can or cannot be detected, respectively.

$$\xi = \frac{n_{\text{FSC}}}{n_0} \sin \beta \quad (7)$$

The length of the light path now reads

$$L(\xi, d) \propto \frac{d}{\sqrt{1 - \xi^2}} \quad (8)$$

and the average number N of total internal reflection events at the surface is given by

$$N(\xi, d) \propto \frac{\xi \cdot d}{h \sqrt{1 - \xi^2}} \quad (9)$$

with h representing the height of the FSC. With increasing detection angle β and distance from the FSC's edge d , the number of total internal reflections at the surfaces increases more strongly than the length of the light path. Thus, a separation of surface and bulk scattering is possible, but will not be presented in this publication. According to this separation, the quality of the FSC's surface is crucial for collecting the fluorescence at the edge. For instance, the loss of fluorescence as a function of β is larger than the loss of fluorescence as a function of d , as shown in Figure 5. Comparing both types of FSC designs, it turns out that the relative loss of fluorescence in the Rh6G sample with spin-coated PMMA matrix is remarkably larger than in both FROT samples, which show a more similar behavior.

5. CONCLUSION

We have developed a simple two-dimensional model to describe the propagation of fluorescence light for a certain FSC device geometry. The asymmetry of the device results in an asymmetry of the angle dependence of fluorescence light; for locally selective illumination, there are regimes of angles under which light is emitted.

The comparison of experimental data with results from numerical modeling confirms the suitability of our ray optics approach that neglects the reemission of fluorescence photons. We conclude that for sufficiently low dye concentration in the FSC photon recycling and elastic scattering of photons exhibit only marginal contribution to the edge emission. Because the contrast of the measured fringe-like pattern (Figure 8) is lower than expected, we think this discrepancy might allow an access to describe the scattering at the surfaces. To distinguish scattering due to the matrix from scattering due to the surfaces, we could illuminate the FSC by light outside the absorption range of the dye [6] and by investigation of FSCs of different thicknesses.

Furthermore, our experiments revealed that the asymmetrically emitted light at the edge of the FSC can also occur, if the fluorescence dye concentration is too high, and hence, the emission of fluorescence light is no longer homogeneously distributed across the depth of the

FSC. With the exactly known photon flux of the first generation fluorescence and the fluorescence at the edge, angle-dependent measurements under local illumination would allow for a calculation of the reabsorption as a function of light path length as well.

ACKNOWLEDGEMENTS

The authors like to thank T. Markvart and N. Soleimani from the School of Engineering Sciences at the University of Southampton for preparing thin film fluorescence collectors and gratefully acknowledge funding by BMBF contract 03SF0332-D.

REFERENCES

1. Weber WH, Lambe J. Luminescent greenhouse collector for solar radiation. *Applied Optics* 1976; **14**: 123–139.
2. Goetzberger A, Greubel W. Solar energy conversion with fluorescent collectors. *Applied Physics* 1977; **12**: 123–139.
3. Viehmann W, Frost RL. Thin film waveshifter coatings for fluorescent radiation converters. *Nuclear Instruments and Methods* 1979; **167**: 405–415.
4. Danos L, Kittidachachan P, Meyer TJJ, Greef R, Markvart T. Characterisation of fluorescent collectors based on solid, liquid and Langmuir Blodgett (LB) films. *Proceedings of 21st European Photovoltaic Solar Energy Conference*, Dresden. 2006; 443–446.
5. Goldschmidt JC, Peters M, Prönneke L, Steidl L, Zentel R, Bläsi B, Gombert A, Glunz S, Willeke G, Rau U. Theoretical and experimental analysis of photonic structures for fluorescent concentrators with increased efficiencies. *Physica Status Solidi A* 2008; **205**: 2811–2821.
6. Sträter H. Spektral- und winkelaufgelöste emission von fluoreszenzkollektoren. Master Thesis, University of Oldenburg, Institute of Physics, Germany 2010.